1. Amine SOBH[1], 2. Belkacem BELABBAS[1], 3. Tayeb ALLAOUI[1]

Laboratory of Energy Engineering and Computer Engineering, Electrical Engineering Department, University of Tiaret, Algeria (1)
ORCID: 2. 0000-0001-7811-8066; 3. 0000-0001-9295-073X

doi:10.15199/48.2024.08.43

Utilizing a Five-Level Inverter for Grid-Connected PV Systems: Implementing an MPPT Algorithm with Super Twisting Sliding Mode Control

***Abstract**. This study highlights the effectiveness of a Super Twisting Sliding Mode Control (STSMC) type nonlinear controller based on Lyapunov stability to improve the ability to extract optimal power under varying weather conditions from the algorithm maximum power point tracking (MPPT). Additionally, this study investigates the benefits of using a multi-level inverter in a grid-connected photovoltaic (PV) energy conversion system. The studied system consists of a PV generator associated with a voltage rise chopper controlled by an MPPT algorithm based on the STSMC controller. Then, the energy generated by the PV system is injected into the electrical grid via a three-phase level three inverter. The results of the simulations carried out using the MATLAB/Sim software showed that the system exhibited good performance in terms of the quality of the energy generated by the PV system and the energy extraction efficiency for data variable weather*

***Streszczenie.** Badanie to podkreśla skuteczność nieliniowego kontrolera typu Super Twisting Sliding Mode Control (STSMC) opartego na stabilności Lapunowa w celu poprawy zdolności do wydobywania optymalnej mocy w różnych warunkach pogodowych z algorytmu śledzenia punktu maksymalnej mocy (MPPT). Ponadto w badaniu tym zbadano korzyści płynące z zastosowania falownika wielopoziomowego w podłączonym do sieci systemie konwersji energii fotowoltaicznej (PV). Badany system składa się z generatora fotowoltaicznego połączonego z czoperem wzrostu napięcia sterowanym algorytmem MPPT opartym na sterowniku STSMC. Następnie energia generowana przez system fotowoltaiczny jest wprowadzana do sieci elektrycznej za pośrednictwem trójfazowego falownika poziomu trzeciego. Wyniki symulacji przeprowadzonych z wykorzystaniem oprogramowania MATLAB/Sim wykazały, że system wykazał się dobrymi parametrami w zakresie jakości energii generowanej przez system PV oraz efektywności pozyskiwania energii dla danych o zmiennej pogodzie. (**Wykorzystanie falownika pięciopoziomowego w systemach fotowoltaicznych podłączonych do sieci: wdrażanie algorytmu MPPT ze sterowaniem w trybie Super Twisting Sliding**)*

Keywords: Photovoltaic energy; multilevel converters; Super Twisting Sliding Mode Control; quality energy.
Słowa kluczowe: Energia fotowoltaiczna; konwertery wielopoziomowe; Kontrola trybu Super Twisting Sliding; jakość energii.

Introduction

The increasing concern over the fluctuating cost of fossil fuels and the deteriorating state of the global environment has led to a growing interest in Renewable Energy Systems (RES) [1].

Photovoltaic power generation is considered the most promising renewable energy technology due to its various advantages such as requiring less maintenance, generating no noise, being clean, smaller in size, and being installable closer to the load centers. However, the efficiency of this technology is highly dependent on weather conditions [2].

The maximum amount of power that can be harnessed from a PV system is determined by various parameters, including temperature and illumination. To extract the maximum power from the available PV energy, Maximum Power Point Tracking (MPPT) algorithms have been developed [3].

However, traditional control strategies such as the Perturb and Observe (P&O) algorithm and incremental conductance can have drawbacks such as complexity, robustness, and difficulty in implementation [4], [5].

To overcome these limitations and achieve maximum energy conversion efficiency, researchers have turned to nonlinear controllers, Artificial Intelligence (AI) approaches, and Neural Networks (NN) [6]-[9].

Among the nonlinear controllers, Sliding Mode Controller (SMC) has been widely applied due to its insensitivity to variations in parameters, stability, simplicity of implementation, and fast response. However, it suffers from the chattering phenomenon [10].

To address this problem, various approaches such as the Second Order Sliding Mode Controller (SOSMC), Fuzzy Sliding Mode Controller (FSMC), and Super-Twisting Sliding Mode Controller (STSMC) have been proposed. In this study, the STSMC is utilized for the MPPT algorithm.

In PV applications, different power converter topologies have been proposed for power conditioning. Multilevel converters, particularly the Neutral Point Clamped (NPC) topology, are commonly used in high-voltage, high-power PV systems. Despite their advantages, these converters face a major issue with balancing capacitor voltages in the DC bus link. To solve this problem, two-loop control algorithms have been proposed, where the outer closed loop controls the average value of the DC voltage using the classical PI, and the inner loop controls the difference between the two voltages in each half using a clamping bridge circuit.

The primary accomplishments of the work can be summarized as follows: First, the implementation of an MPPT algorithm based on STSMC was carried out to ensure the optimal extraction of PV power. Second, the use of multilevel converters led to an enhancement of PV power quality. Lastly, the work ensured energy stability between the production sources (Grid and PV) and the load.

In Section 2, the studied system is globally modelled. Section 3 focuses on the control strategy of the Five-Level NPC Inverter and introduces an STSMC control design for the MPPT Algorithm. Section 4 showcases the results obtained and provides an explanation. Finally, Section 5 presents the conclusion of this work.

Methods

Fig. 1 displays the PV system that is linked to the power grid. To extract the maximum power, the GPV is connected to the DC bus by means of a voltage booster chopper that is regulated by an MPPT algorithm. Afterward, the system is linked to the power grid using a five-level inverter. To eliminate the high-frequency harmonics caused by the switching of the static switches, a passive filter RL is connected between the output of the inverter and the grid.

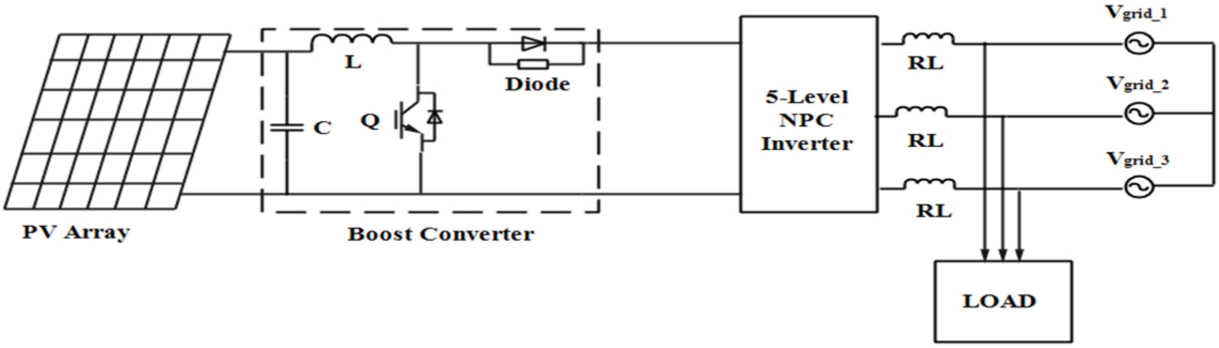

Fig.1. Proposed PV system connected to the grid.

PV Array Model

Fig. 2 illustrates the PV cell that was utilized in this study. The modeling of this solar cell is thoroughly presented in [12].

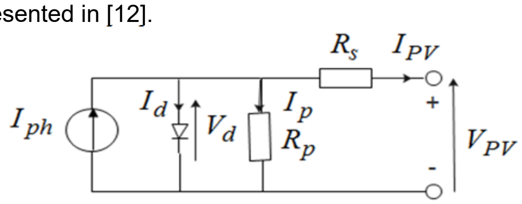

Fig.2. PV cell circuit model.

Boost Converter

Fig. 3 displays the electrical circuit diagram of the boost converter which comprises an inductor L_1 and a capacitor C_1. As a result, the output voltage of the boost converter can be determined as follows:

(1) $$V_0 = \frac{V_{IN}}{(1-\alpha)}$$

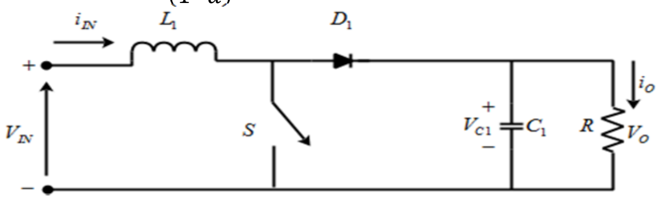

Fig.3. Boost converter.

Five Level NPC Inverter

The topology of the five-level NPC converter is shown in Fig. 4. It consists of four serial capacitors $(V_{C1}, V_{C2}, V_{C3}, V_{C4})$ forming a midpoint (M). This structure consists of three arms K $(K = A, B$ or $C)$. Each of the three arms is composed of eight controlled switches $(T_{i1}, T_{i2}, T_{i3}, T_{i4}, T_{i5}, T_{i6}, T_{i7}, T_{i8})$ and two clamping diodes (DD_{i1}, DD_{i2}). The modeling of the five-level NPC inverter is discussed in more detail in [1].

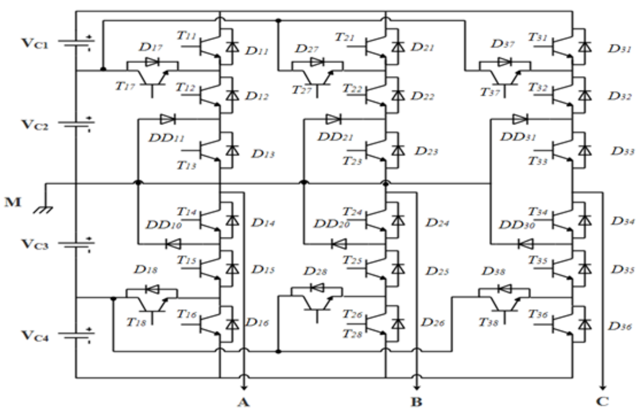

Fig.4. Topology of the five-level NPC inverter.

Control strategies

This section provides a detailed description and design steps of the different control strategies for PV system.

STSMC design for MPPT algorithm

This section introduces the fundamental principle and design process of the MPPT algorithm utilizing STSMC. This algorithm successfully overcomes chattering, a common drawback in conventional SMC (Sliding Mode Control), while maintaining the same level of robustness and tracking performance as the conventional method. [2].

The STSMC scheme consists of two terms: the equivalent control U_{equ} and super twisting control U_{st}.

(2) $$u(t) = u_{equ}(t) + u_{st}(t)$$

(3) $$u_{st}(t) = u_1(t) + u_2(t)$$

(4) $$\begin{cases} u_1(t) = -\lambda . |S|^{1/2} . sgn\,(S) \\ \dot{u}_2(t) = -\gamma . sgn(S) \end{cases}$$

Where λ and γ are the positive constants and the fixed-gain can chose as:

(5) $$\begin{cases} \lambda > \frac{\Phi}{\Gamma_{min}} \\ \gamma^2 \geq \frac{4.\Phi}{\Gamma_{min}^2} . \frac{\Gamma_{max}(\lambda-\Phi)}{\Gamma_{min}(\lambda-\Phi)} \end{cases}$$

With: Φ, Γ_{min}, Γ_{max} are the positive constants.

To achieve equivalent control in STSMC, the design procedure is identical to that of conventional SMC. The following steps are involved in the design process of an MPPT algorithm utilizing STSMC:

Equivalent control

The switching surface is designed as:

(6) $$S = \frac{\partial P_{PV}}{\partial V_{PV}} = \frac{\partial (V_{PV}.I_{PV})}{\partial V_{PV}}$$

(7) $$S = I_{PV} + V_{PV}\frac{\partial I_{PV}}{\partial V_{PV}}$$

(8) $$S = V_{PV}\left(\frac{\partial I_{PV}}{\partial V_{PV}} + \frac{I_{PV}}{V_{PV}}\right)$$

(9) $$S = V_{PV}\left(\frac{I_{PV}(k)-I_{PV}(k-1)}{V_{PV}(k)-V_{PV}(k-1)} + \frac{I_{PV}(k)}{V_{PV}(k)}\right)$$

The PV output power is controlled by adjusting the duty cycle α of the boost converter. Thus, the equivalent control given by:

(10) $$U_{equ}(t) = \alpha = 1 - \frac{V_{in}}{V_o}$$

Super-Twisting Control (STC)

In this work, the hyperbolic tangent surface is used for the STC due to its robustness and fast convergence. For the STC terms can written as:

(11) $U_{st}(t) = -\lambda . |S|^{1/2} . tanh\,(S) - \int \gamma . tanh(S) . dt$

The positive gains for λ and γ are chosen to fulfil the condition of convergence.

Five-Level NPC Inverter

The imbalance of input voltages in the five-level inverter can result in a floating-point potential issue. Moreover, for the smooth operation of the inverter with five levels, it is essential that these four input voltages remain constant and equal. To maintain the stability of the DC bus voltages, minimizing the voltage difference between them is crucial. The Clamping Bridge, a balancing bridge structure commonly used in multilevel converters, has been proposed in the literature. It consists of a transistor and a resistor (R_p) in series that are placed parallel to the terminals of each capacitor on the DC bus, as illustrated in Fig. 5. Each transistor is controlled to maintain the input voltages of the inverter at a fixed reference value. In this scenario, the mathematical model of the DC bus incorporating the clamping bridge can be defined as follows.

$$(12)\quad \begin{cases} C_1 \frac{dV_{c1}}{dt} = I_{rec1} - I_{r1} - I_{l1} \\ C_2 \frac{dV_{c2}}{dt} = I_{rec1} + I_{rec2} - I_{r2} - I_{l1} - I_{l2} \\ C_3 \frac{dV_{c3}}{dt} = -I_{rec3} - I_{rec4} - I_{r3} + I_{l3} + I_{l4} \\ C_4 \frac{dV_{c4}}{dt} = -I_{rec4} - I_{r4} + I_{l4} \end{cases}$$

With:

$$I_{ri} = \frac{V_{ci}}{R_p}; i = [1\ 4]$$

The control algorithm for the clamping bridge involves real-time comparison of the differences (ΔU_{12}) and (ΔU_{34}) in the continuous voltages of each stage with zero values. If the difference is non-zero, the surplus energy is dissipated via the resistance. The control algorithm for the clamping bridge can be expressed as follows:

$$(13)\quad \begin{cases} \Delta V_{12} > 0 \Rightarrow I_{r1} = 0\ \&\ I_{r2} \neq 0\ (T_1 = 0\ \&\ T_2 = 1) \\ \Delta V_{12} < 0 \Rightarrow I_{r1} \neq 0\ \&\ I_{r2} = 0\ (T_1 = 1\ \&\ T_2 = 0) \\ \Delta V_{34} > 0 \Rightarrow I_{r3} = 0\ \&\ I_{r4} \neq 0\ (T_3 = 0\ \&\ T_4 = 1) \\ \Delta V_{34} < 0 \Rightarrow I_{r3} \neq 0\ \&\ I_{r4} = 0\ (T_2 = 1\ \&\ T_4 = 0) \end{cases}$$

With: $\Delta V_{12} = V_{c1} - V_{c2}; \Delta V_{34} = V_{c3} - V_{c4}$

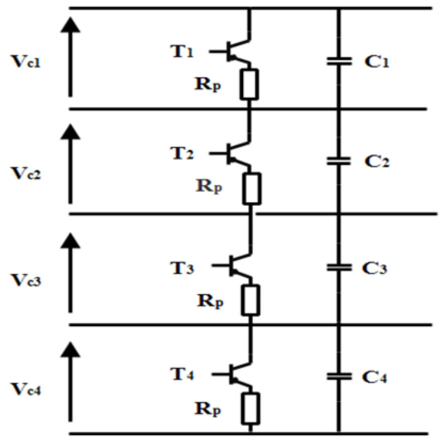

Fig.5. DC bus voltage control loop.

Control of the Injected Powers

Multiple strategies exist for controlling active and reactive powers, but the instantaneous power method is commonly utilized in production systems to manage the active and reactive powers supplied to the power grid.

The power control scheme is shown in Fig. 6. The PWM technique is used to control the five-level inverter.

The active and reactive powers in the Concordia coordinate system are determined using the following two equations:

$$(14)\quad \begin{cases} P = \frac{3}{2}(V_\alpha I_\alpha + V_\beta I_\beta) \\ Q = \frac{3}{2}(V_\beta I_\alpha - V_\alpha I_\beta) \end{cases}$$

The reference currents are calculated according to the following equation system:

$$(15)\quad \begin{cases} i_\alpha^* = \frac{2}{3}\left(\frac{P.V_\alpha + Q.V_\beta}{V_\alpha^2 + V_\beta^2}\right) \\ i_\beta^* = \frac{2}{3}\left(\frac{P.V_\beta - Q.V_\alpha}{V_\alpha^2 + V_\beta^2}\right) \end{cases}$$

By injecting only, the active power generated by the photovoltaic generator for the purpose of ensuring a unit power factor. It is imposed that the reactive power injected is equal to zero $(Q^* = 0)$. Equation 14 becomes:

$$(16)\quad \begin{cases} i_\alpha^* = \frac{2}{3}\left(\frac{P.V_\alpha}{V_\alpha^2 + V_\beta^2}\right) \\ i_\beta^* = \frac{2}{3}\left(\frac{P.V_\beta}{V_\alpha^2 + V_\beta^2}\right) \end{cases}$$

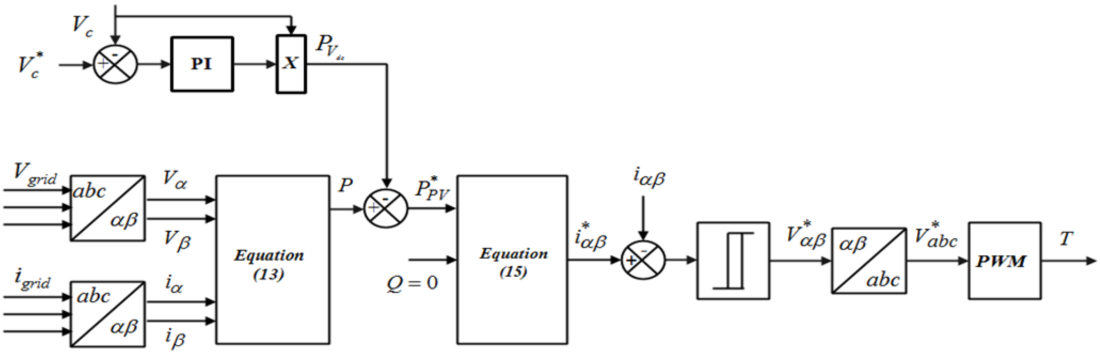

Fig.6. Control block diagram of the injection process.

Results and discussion

This section reports on the simulation results obtained from integrating the PV system with the electric grid using MATLAB/Sim Power System software. The simulations were conducted under solar illumination conditions of $G = 1000\ [W/m^2]$ and a temperature of $T = 293$ [K].

Tables 1 and 2 detail the system settings used in the simulations.

Table 1. Parameters of the PV cell (MODEL KC200GT)

P_{PV}	W	200.143
$V_{oc,n}$	V	32.9
$I_{sc,n}$	A	8.21
$I_{0,n}$	A	$9.825.10^{-8}$
R_p	Ω	415.405
R_s	Ω	0.221
K_V	V/K	-0.123
K_I	A/K	0.0032
a	-	1.3
N_s	-	54
K	J/K	$1.381.10^{-23}$
q	C	$1.602.10^{-19}$

Table 2. Boost Converter Parameters

L	mH	1.21
C	µF	2200

Fig. 7 illustrates the load, grid, and PV power distribution in response to varying loads. The simulations show that the PV generates a constant power, and to maintain energy stability between the PV source and the load, the power grid must adapt to the load variation at all times, as per the meteorological data.

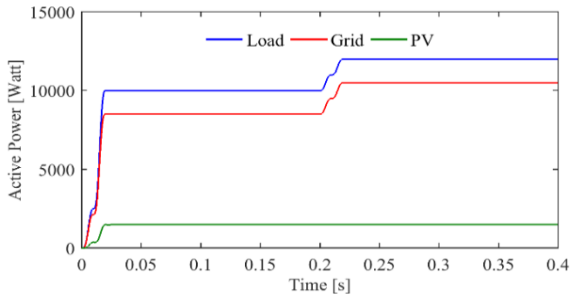

Fig.7. Active power of the Load, Grid and GPV.

Fig. 8 illustrate the sinusoidal waveforms of the load (a), electric grid (b), and PV (c) currents, all operating at a frequency of 50 Hz.

Additionally, Fig. 9 displays the root-mean-square (RMS) values of the three currents under various load conditions, with the direction of the currents determined by an equation.

$$i_{Load} = i_{Grid} + i_{PV} \tag{17}$$

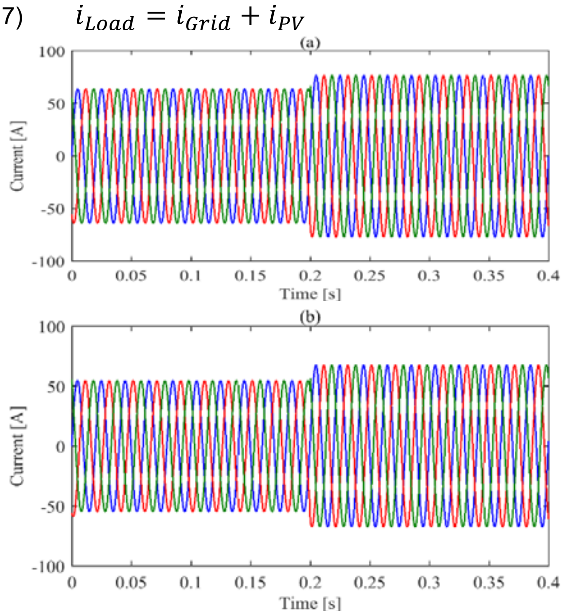

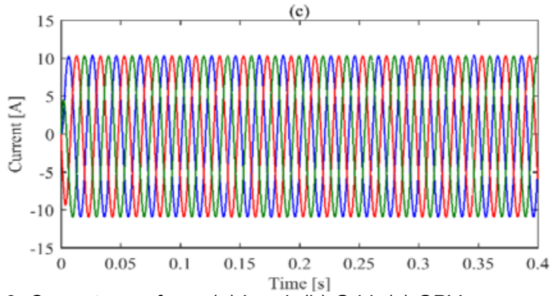

Fig.8. Current waveform: (a) Load, (b) Grid, (c) GPV.

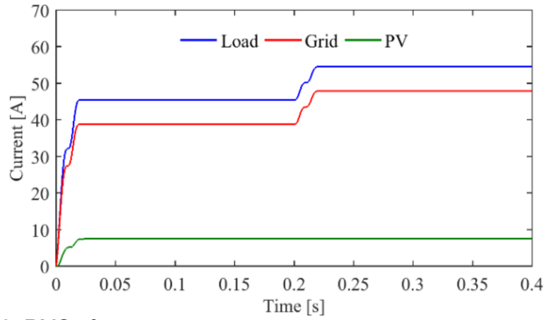

Fig.9. RMS of currents.

The total harmonic distortion (THD) of the load (a), electric grid (b), and PV (c) currents is analysed in Fig. 10, with all three currents exhibiting THD values of less than 5%. These findings indicate that using a five-level inverter enhances the energy quality produced by the PV system while leaving the quality of the energy supplied by the grid unaffected.

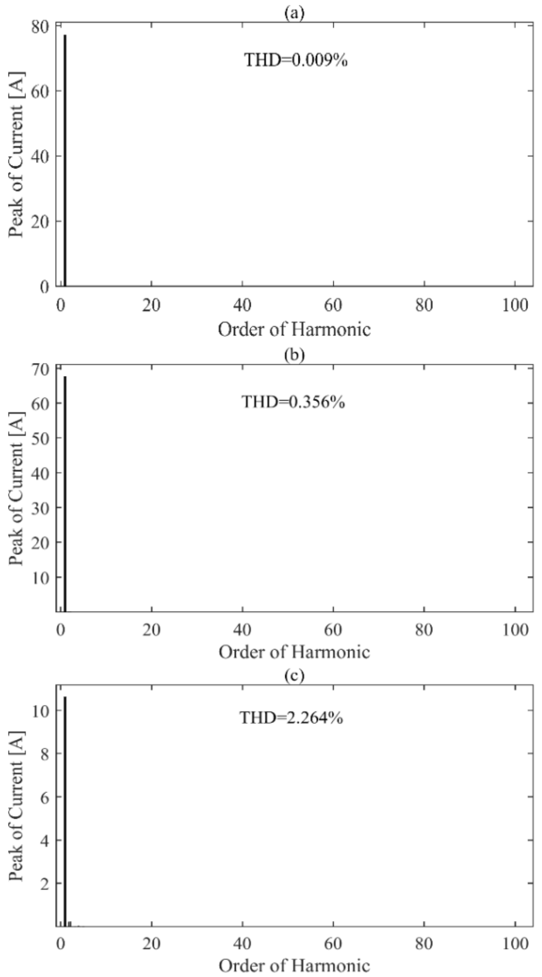

Fig.10. THD: (a) Load, (b) Grid, (c) GPV.

The DC bus voltage control structure functions accurately, as shown in Fig. 11, where the measured voltage successfully tracks its reference, without any impact on load variation.

Finally, Fig. 12 depicts the waveform of the five-level inverter's compound voltage, with five voltage levels indicating the converter's use.

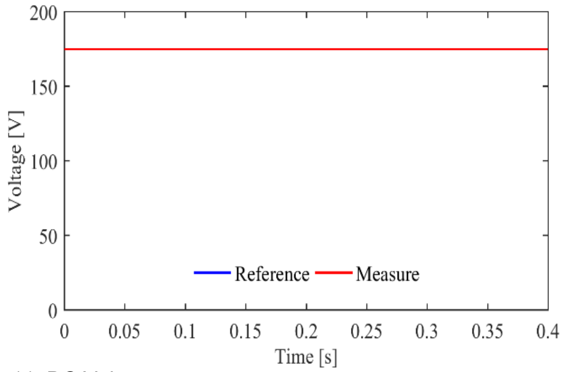

Fig.11. DC Voltage.

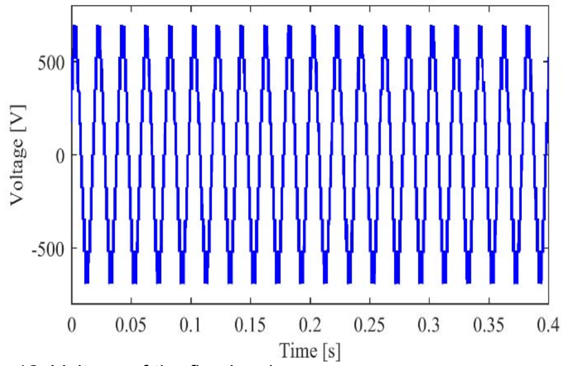

Fig.12. Voltage of the five-level.

Conclusions

In this study, our objective was twofold: to maximize the electric power extracted from a PV energy source using an MPPT algorithm controlled by STSMC, and to enhance the quality of the energy produced by incorporating a five-level inverter into the energy conversion process. Through qualitative simulations, we were able to demonstrate the benefits of using this inverter with STSMC. Our results clearly indicate that the MPPT algorithm employed in this study is highly efficient in extracting maximum energy and that the use of a five-level inverter significantly improves the quality of energy generated by the PV.

Authors

Amine SOBH, Laboratory of Energy and Computer Engineering (L2GEGI), Department of Electrical Engineering, Faculty of Sciences Applied, University Ibn Khaldoun of Tiaret, BP 78 Size Zarroura, Tiaret 14000, Algeria, sobh.amine@univ-tiaret.dz

Belkacem BELABBAS, Laboratory of Energy and Computer Engineering (L2GEGI), Department of Electrical Engineering, Faculty of Sciences Applied, University Ibn Khaldoun of Tiaret, BP 78 Size Zarroura, Tiaret 14000, Algeria, belabbas.belkacem@univ-tiaret.dz

Tayeb ALLAOUI, Laboratory of Energy and Computer Engineering (L2GEGI), Department of Electrical Engineering, Faculty of Sciences Applied, University Ibn Khaldoun of Tiaret, BP 78 Size Zarroura, Tiaret 14000, Algeria, tayeb.alaoui@univ-tiaret.dz

REFERENCES

[1] H.-L. Jou, Y.-H. Chang, J.-C. Wu, and K.-D. Wu, “Operation strategy for a lab-scale grid-connected photovoltaic generation system integrated with battery energy storage,” Energy Convers. Manag., vol. 89, pp. 197–204, Jan. 2015.

[2] A. Hebib, T. Allaoui, A. Chaker, B. Belabbas, and M. Denai, ‘A comparative study of classical and advanced MPPT control algorithms for photovoltaic systems’, Przegląd Elektrotechniczny, vol. 96, 2020..

[3] S. Alagammal and N. Rathina Prabha, ‘Combination of modified P&O with power management circuit to exploit reliable power from autonomous PV-battery systems’, Iran. J. Sci. Technol. Trans. Electr. Eng., vol. 45, no. 1, pp. 97–114, 2021.

[4] S. H. Sheikh Ahmadi, M. Karami, M. Gholami, and R. Mirzaei, ‘Improving MPPT Performance in PV Systems Based on Integrating the Incremental Conductance and Particle Swarm Optimization Methods’, Iran. J. Sci. Technol. Trans. Electr. Eng., vol. 46, no. 1, pp. 27–39, 2022.

[5] C.-M. Hong and C.-H. Chen, “Intelligent control of a grid-connected wind-photovoltaic hybrid power systems,” Int. J. Electr. Power Energy Syst., vol. 55, no. Supplement C, pp. 554–561, Feb. 2014.

[6] A. Kchaou, A. Naamane, Y. Koubaa, and N. M’sirdi, “Second order sliding mode-based MPPT control for photovoltaic applications,” Sol. Energy, vol. 155, pp. 758–769, 2017.

[7] B. Yang et al., “Perturbation observer based fractional-order sliding-mode controller for MPPT of grid-connected PV inverters: Design and real-time implementation,” Control Eng. Pract., vol. 79, pp. 105–125, 2018.

[8] M. Arsalan, R. Iftikhar, I. Ahmad, A. Hasan, K. Sabahat, and A. Javeria, “MPPT for photovoltaic system using nonlinear backstepping controller with integral action,” Sol. Energy, vol. 170, pp. 192–200, 2018.

[9] N. Karami, N. Moubayed, and R. Outbib, “General review and classification of different MPPT Techniques,” Renew. Sustain. Energy Rev., vol. 68, pp. 1–18, 2017.

[10] M. Farhat, O. Barambones, and L. Sbita, “A new maximum power point method based on a sliding mode approach for solar energy harvesting,” Appl. Energy, vol. 185, pp. 1185–1198, 2017.

[11] B. Belabbas, T. Allaoui, M. Tadjine, and M. Denai, “Power Quality Enhancement in Hybrid Photovoltaic-Battery System based on three–Level Inverter associated with DC bus Voltage Control,” J. Power Technol., vol. 97, no. 4, pp. 272–282, 2017.

[12] B. Belabbas, T. Allaoui, M. Tadjine, and M. Denai, “Power management and control strategies for off-grid hybrid power systems with renewable energies and storage,” Energy Syst., pp. 1–30, 2017.

[13] J. Li, Z. Pan, and R. Burgos, “A new control scheme of five-level active NPC converters for common mode voltage mitigation in medium voltage drives,” in 2014 IEEE Energy Conversion Congress and Exposition (ECCE), 2014, pp. 234–241.